

Supporting Information

Sequence determinants of a D-Tetra-Peptide vaccine adjuvant effect

Yiming Zhang¹, Zhiwen Hu¹, Xinxin Li¹, Yinghao Ding¹, Zhenghao Zhang¹,
Xiangyang Zhang¹, and Wenting Zheng^{2*}, Zhimou Yang^{1*}

¹ College of Life Sciences, Key Laboratory of Bioactive Materials, Ministry of Education, and Collaboration Innovation Center of Chemical Science and Engineering (Tianjin), Nankai University, Tianjin 300071, P.R. China

² State Key Laboratory of Experimental Hematology, National Clinical Research Center for Blood Diseases, Institute of Hematology & Blood Diseases Hospital, Chinese Academy of Medical Sciences & Peking Union Medical College, Tianjin 300020, China

Correspondence and requests for materials should be addressed to email:

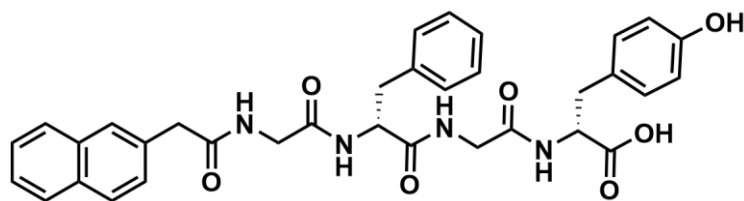
zhengwenting@ihcams.ac.cn; yangzm@nankai.edu.cn

Materials and method

Peptides synthesis and characterizations:

Preparation of peptides: All peptides were prepared by standard solid phase peptide synthesis (SPPS) by using 2-chlorotrityl chloride resin and the corresponding N-Fmoc protected amino acids with side chains properly protected. Firstly, the C-terminal of the first amino acid was conjugated on the resin. Anhydrous N,N'-dimethylformamide (DMF) containing 20% piperidine was used to remove Fmoc protected group. To couple the next amino acid to the free amino group, O-Benzotriazol-1-yl-N,N,N',N'-tetramethyluronium hexafluorophosphate (HBTU) was used as coupling reagent. Peptides chain was extended according to the standard SPPS protocol. NSAIDs were used at the final step. Lastly, 95% TFA containing 2.5% H₂O and 2.5% TIS was used to cleave peptides derivative from resin and the mixture was filtered. Ice cold diethyl ether was poured into filtrate concentrated by rotary evaporation. The precipitate was centrifuged for 5 min at 5000 rpm speed. The solid was dried by vacuum pump and then purified by HPLC to obtain the pure compounds.

Characterization of the gelators:



Scheme S1. Chemical structure of Sol-gfgy

Sol-gfgy : $^1\text{H NMR}$ (400 MHz, $\text{DMSO-}d_6$) δ 12.67 (s, 1H), 9.19 (s, 1H), 8.24 (dt, $J = 25.1, 5.7$ Hz, 2H), 8.13 (d, $J = 8.2$ Hz, 1H), 8.04 (d, $J = 8.0$ Hz, 1H), 7.95 – 7.78 (m, 3H), 7.74 (s, 1H), 7.54 – 7.36 (m, 3H), 7.31 – 7.09 (m, 5H), 7.00 (d, $J = 8.2$ Hz, 2H), 6.69 – 6.61 (m, 2H), 4.51 (td, $J = 9.0, 4.3$ Hz, 1H), 4.36 (td, $J = 8.2, 5.2$ Hz, 1H), 3.76 (dd, $J = 16.7, 5.8$ Hz, 2H), 3.69 – 3.55 (m, 4H), 3.01 (dd, $J = 13.9, 4.3$ Hz, 1H), 2.92 (dd, $J = 13.9, 5.3$ Hz, 1H), 2.76 (dt, $J = 13.8, 9.6$ Hz, 2H). MS: calc. $M = 610.24$, obsvd. $(M + H)^+ = 611.24$, $(M + Na)^+ = 633.5148$.

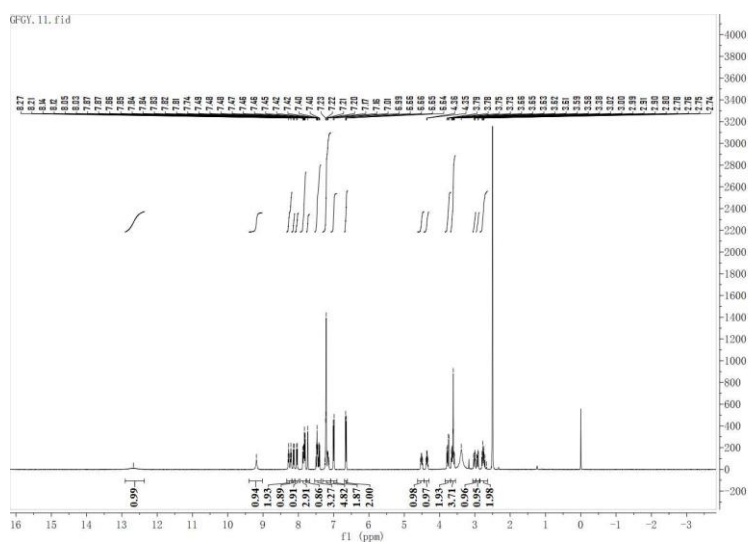


Figure S1. $^1\text{H NMR}$ spectrum of Sol-gfgy

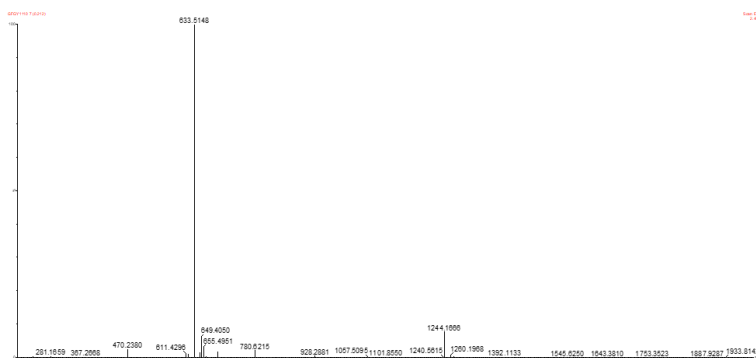
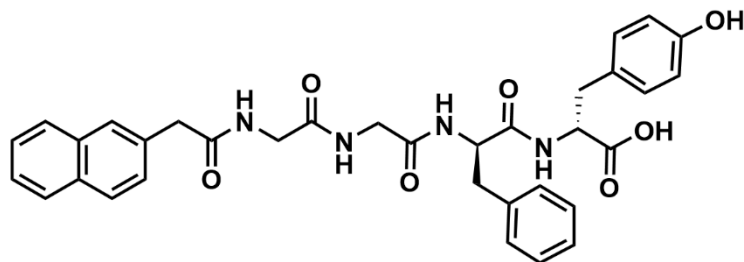


Figure S2. HR-MS spectrum of Sol-gfgy



Scheme S2. Chemical structure of Sol-ggfy

Sol-ggfy: $^1\text{H NMR}$ (400 MHz, $\text{DMSO-}d_6$) δ 12.64 (s, 1H), 9.19 (s, 1H), 8.34 (t, $J = 5.7$ Hz, 1H), 8.24 (d, $J = 7.8$ Hz, 1H), 8.05 (t, $J = 5.7$ Hz, 1H), 8.00 (d, $J = 8.5$ Hz, 1H), 7.89 – 7.79 (m, 3H), 7.46 (dddd, $J = 11.6, 10.1, 6.6, 1.7$ Hz, 4H), 7.22 (d, $J = 5.7$ Hz, 5H), 7.06 – 6.98 (m, 2H), 6.70 – 6.61 (m, 2H), 4.54 (td, $J = 9.0, 3.9$ Hz, 1H), 4.35 (td, $J = 8.1, 5.4$ Hz, 1H), 3.77 – 3.51 (m, 7H), 2.96 (ddd, $J = 18.9, 13.9, 4.7$ Hz, 2H), 2.88 – 2.79 (m, 1H), 2.78 – 2.63 (m, 1H). MS: calc. $M = 610.24$, obsvd. $(M + H)^+ = 611.24$, $(M + Na)^+ = 633.4798$.

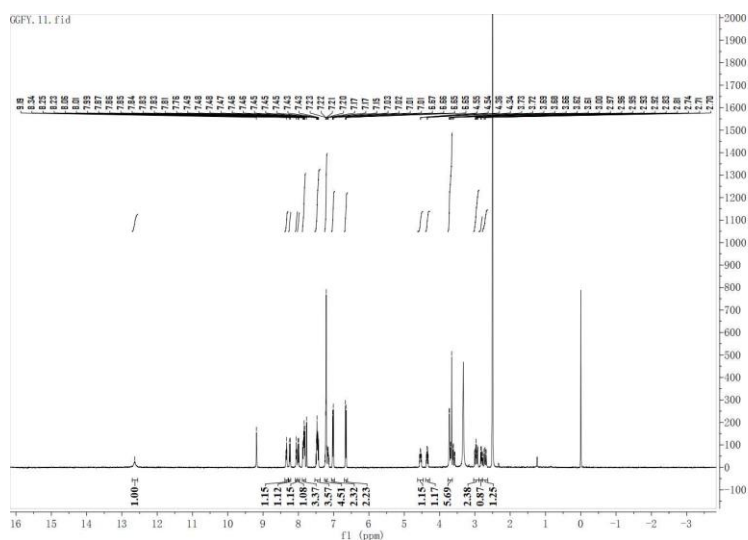


Figure S3. $^1\text{H NMR}$ spectrum of Sol-ggfy

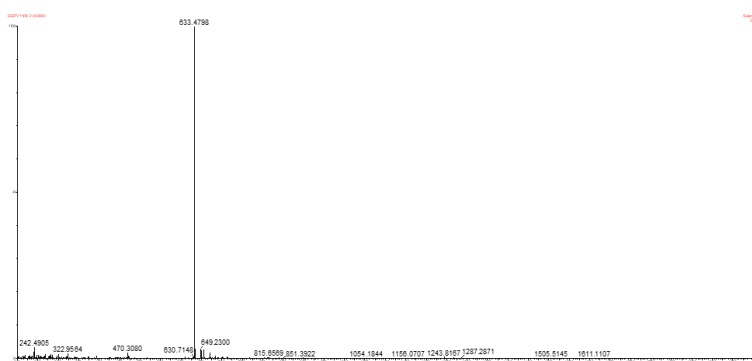
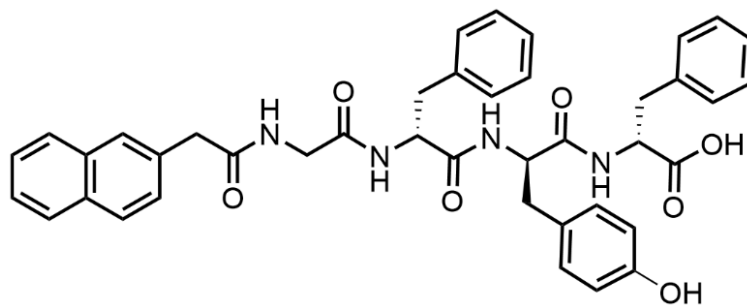


Figure S4. HR-MS spectrum of Sol-ggfy



Scheme S4. Chemical structure of **Gel-gfyf**

Gel-gfyf: ^1H NMR (400 MHz, $\text{DMSO}-d_6$) δ 12.71 (s, 1H), 9.12 (s, 1H), 8.30 – 8.14 (m, 2H), 8.06 (d, $J = 8.3$ Hz, 1H), 7.99 (d, $J = 8.4$ Hz, 1H), 7.93 – 7.79 (m, 3H), 7.74 (s, 1H), 7.59 – 7.36 (m, 3H), 7.31 – 7.08 (m, 10H), 7.01 (d, $J = 8.2$ Hz, 2H), 6.62 (d, $J = 8.3$ Hz, 2H), 4.47 (dtd, $J = 13.3, 8.5, 4.5$ Hz, 3H), 3.74 – 3.54 (m, 4H), 3.07 (dd, $J = 14.0, 5.4$ Hz, 1H), 2.99 – 2.78 (m, 3H), 2.64 (td, $J = 10.0, 9.5, 4.9$ Hz, 2H). MS: calc. $M = 700.28$, obsvd. $(M + H)^+ = 701.6767$, $(M + \text{Na})^+ = 723.3687$.

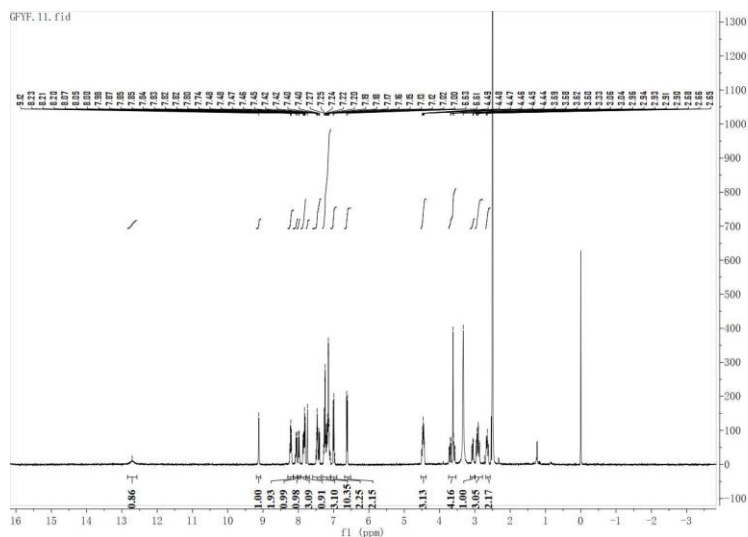


Figure S7. ^1H NMR spectrum of **Gel-gfyf**

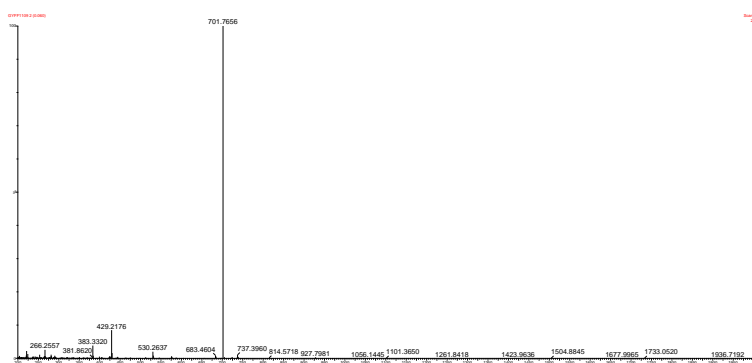
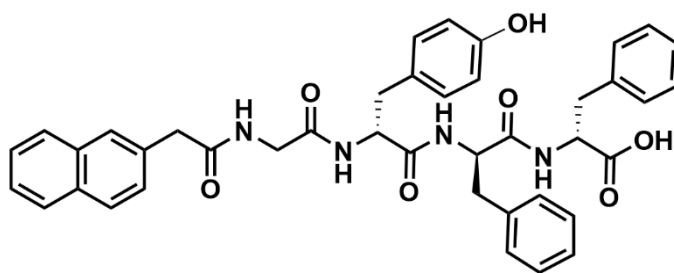


Figure S8. HR-MS spectrum of **Gel-gfyf**



Scheme S5. Chemical structure of **Gel-gyff**

Gel-gyff: ^1H NMR (400 MHz, $\text{DMSO-}d_6$) δ 12.74 (s, 1H), 9.11 (s, 1H), 8.31 – 8.16 (m, 2H), 8.07 (d, $J = 8.3$ Hz, 1H), 7.99 – 7.78 (m, 4H), 7.75 (s, 1H), 7.56 – 7.37 (m, 3H), 7.32 – 7.08 (m, 9H), 6.93 (d, $J = 8.1$ Hz, 2H), 6.59 (d, $J = 8.1$ Hz, 2H), 4.59 – 4.34 (m, 3H), 3.77 – 3.57 (m, 6H), 3.13 – 2.89 (m, 3H), 2.84 – 2.72 (m, 2H). MS: calc. $M = 700.29$, obsvd. $(M + \text{H})^+ = 701.7656$.

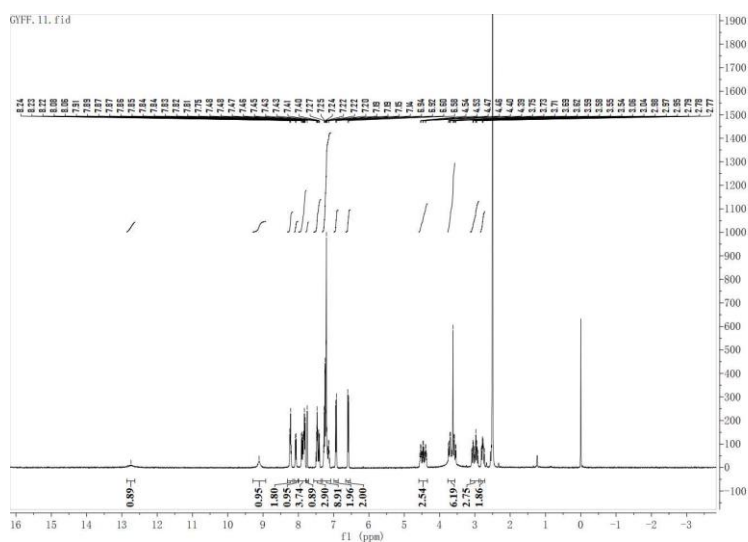


Figure S9. ^1H NMR spectrum of **Gel-gyff**

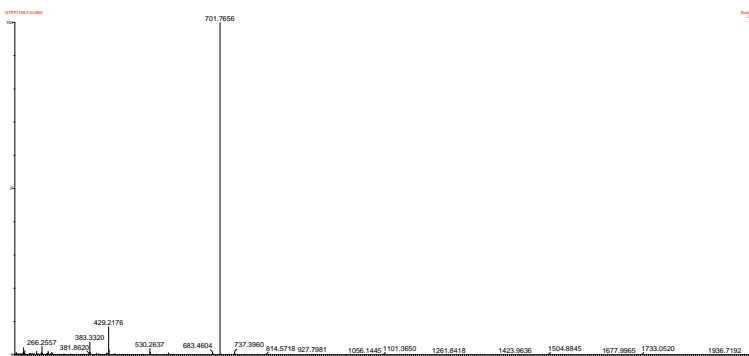
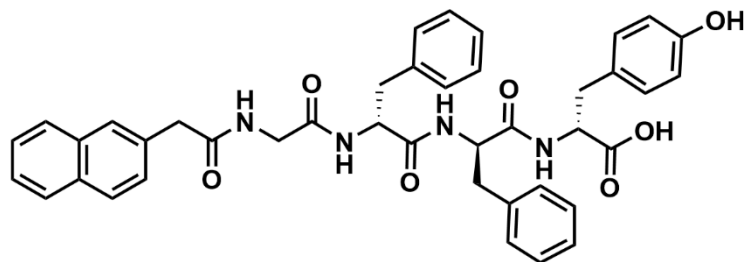


Figure S10. HR-MS spectrum of **Gel-gyff**



Scheme S6. Chemical structure of **Gel-gffy**

Gel-gffy: $^1\text{H NMR}$ (400 MHz, $\text{DMSO-}d_6$) δ 9.19 (s, 1H), 8.29 – 8.07 (m, 3H), 7.98 (d, $J = 8.3$ Hz, 1H), 7.89 – 7.77 (m, 3H), 7.75 (s, 1H), 7.59 – 7.35 (m, 3H), 7.32 – 7.07 (m, 10H), 7.02 (d, $J = 8.2$ Hz, 2H), 6.66 (d, $J = 8.2$ Hz, 2H), 4.59 – 4.42 (m, 1H), 4.42 – 4.33 (m, 1H), 3.71 (dd, $J = 16.9, 5.7$ Hz, 1H), 3.65 – 3.30 (m, 3H), 3.05 – 2.89 (m, 2H), 2.80 (ddd, $J = 23.7, 14.1, 9.0$ Hz, 2H), 2.71 – 2.60 (m, 1H), 2.54 (s, 1H). MS: calc. $M = 700.29$, obsvd. $(M + \text{H})^+ = 701.7656$.

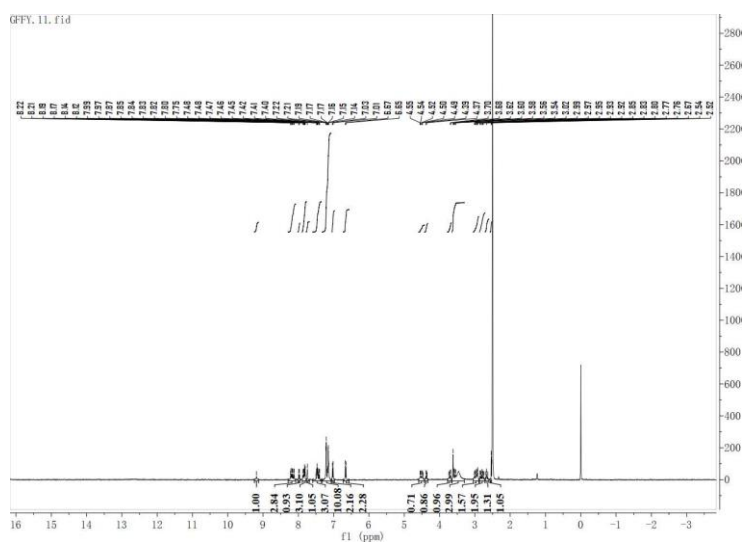


Figure S11. $^1\text{H NMR}$ spectrum of **Gel-gffy**

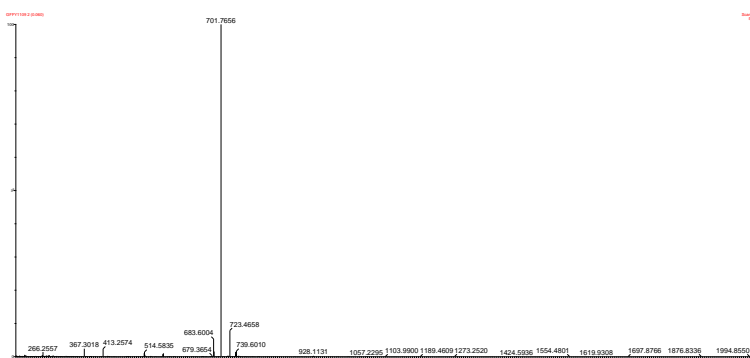


Figure S12. HR-MS spectrum of **Gel-gffy**



Figure S13. The optical photograph of **Sol-gfgy** (2 wt%) and **Sol-ggfy** (2 wt%)

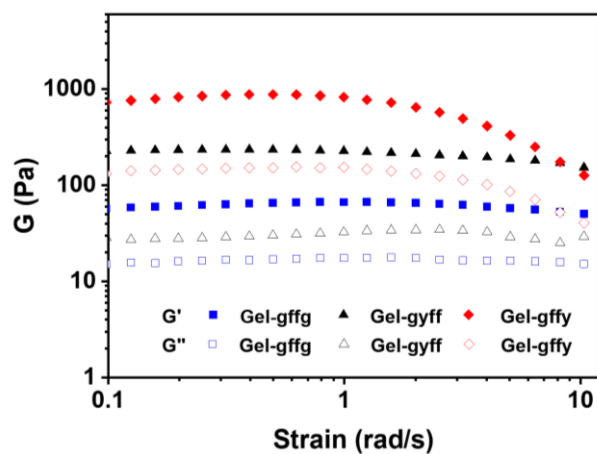


Figure S14. The Oscillatory rheology dynamic strain sweeps of hydrogels **Gel-gffg**, **Gel-gyff** and **Gel-gffy** (2.85 mM).

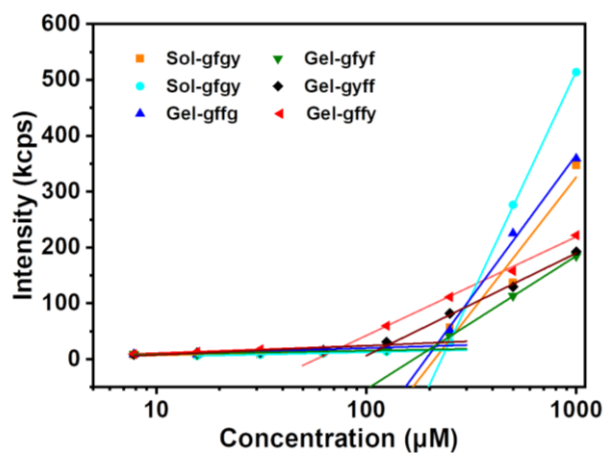


Figure S15. The CAC spectrum of six compounds at the concentration of 2.85 mM.

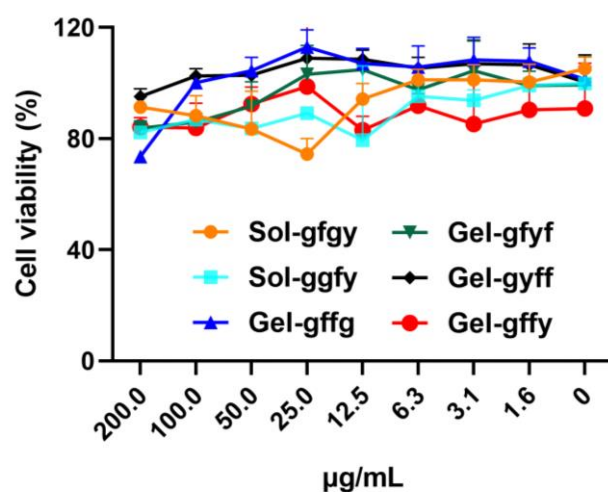


Figure S16. The cytotoxicity effect of empty hydrogel on DC2.4 cells. The DC2.4 (1×10^4 cells/well) were treated with 0-200 $\mu\text{g/mL}$ all compounds for 24 h, and the cytotoxicity was measured using MTT methods. The bars shown are mean \pm SE, $n=3$.

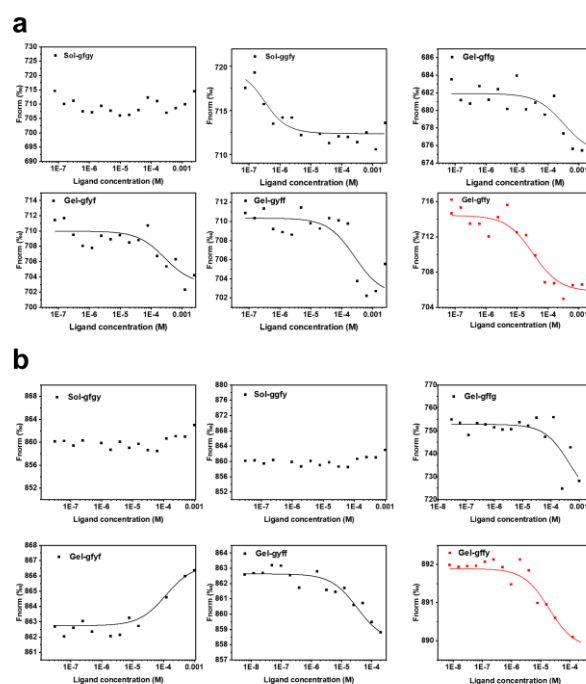


Figure S17. The fitting curve of MST to calculate the K_D value of six compounds to Insulin receptor (a) and IGF-1 receptor (b).

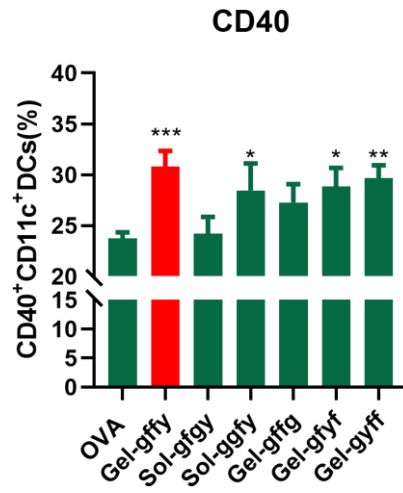


Figure S18. The percent of BMDCs expressing CD40 measured by flow cytometry.

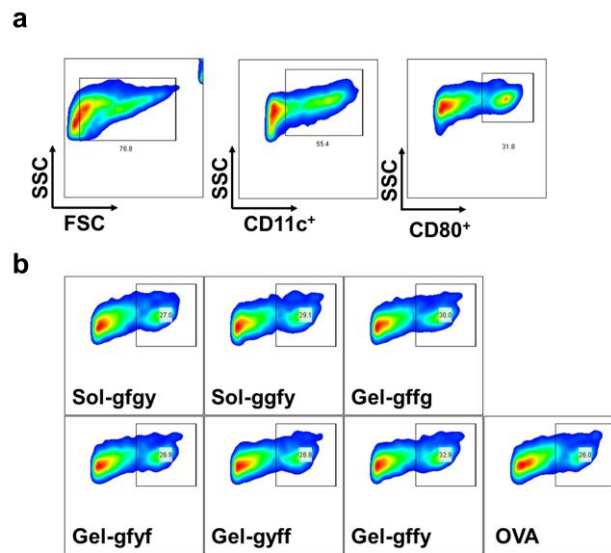


Figure S19. A representative gating strategy of mature BMDCs (a) and the CD80 expression level stimulated by six compounds encapsulated OVA and free OVA (b).

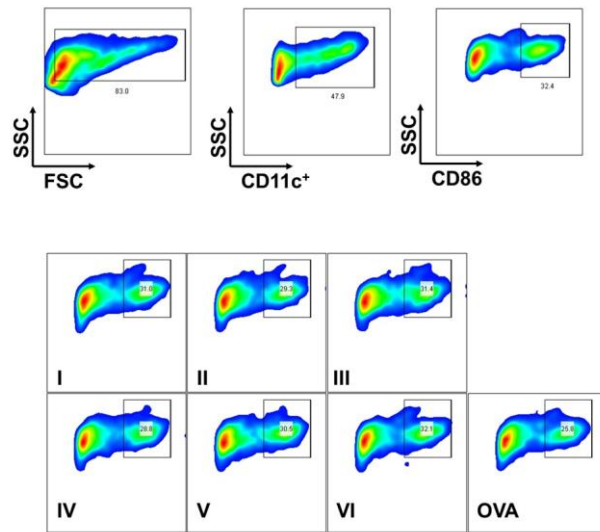


Figure S20. A representative gating strategy of mature BMDCs (a) and the CD86 expression level stimulated by six compounds encapsulated OVA and free OVA (b).

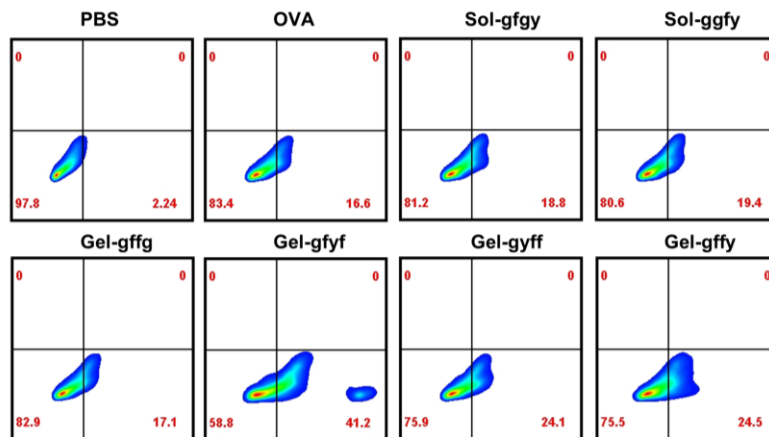


Figure S21. The cellular uptake of BMDCs (1×10^6 cells per well) was incubated with Peptide/FITC-OVA vaccine in a 24-well plate at 37 °C for 2 h.

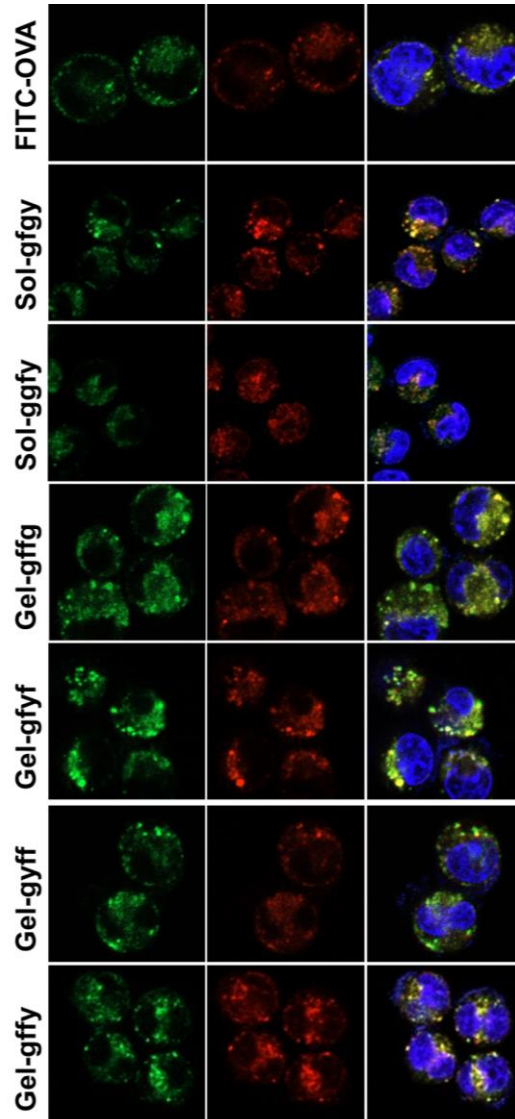


Figure S22. The lysosomal escape of OVA-FITC in DC2.4 after incubation for 4 h was recorded using confocal laser scanning microscopy. Scale bars, 20 μm .